Inorg. Chem. **2002**, *41*, 1761–1770

Structure and Bonding in $[M_6O_{19}]^{n-}$ Isopolyanions

Adam J. Bridgeman*,† and Germán Cavigliasso†,‡

Departments of Chemistry, University of Hull, Kingston upon Hull, HU6 7RX, U.K., and University of Cambridge, Lensfield Road, Cambridge CB2 1EW, U.K.

Received October 22, 2001

The structure and bonding in $[M_6O_{19}]^{n-}$ isopolyanions of Nb, Ta, Mo, and W have been investigated using density-functional methods. The computational–experimental agreement is good for the geometrical parameters of Mo and W species but less satisfactory for Nb and Ta clusters. The electronic structure of the anions has been probed with molecular-orbital, Mulliken–Mayer, and bonding-energy approaches. The results have indicated that M–O interactions are largely M d–O p in character and that σ and π bonds link the metal centers to terminal and bridging (O_b) oxygen atoms. Some M–O_b bonds exhibit a $[M_4O_4]$ closed-loop structure, but this orbital-interaction mode has not been found to make a particularly outstanding contribution to the bonding stability of the molecules. Mayer indexes correspond to (fractional) multiple, approximately single, and low-order character for terminal, bridging, and internal bonds, respectively, and the valency analysis has yielded similar bonding capacities for the different oxygen atoms. A distribution of the negative charge over all types of oxygen sites and metal charges considerably smaller than the formal oxidation states have been obtained from the Mulliken analysis. Minimal structural changes have been detected on reduction of molybdates and tungstates, in accord with the general properties of the orbitals occupied by the added electrons.

Introduction

Polyoxometalates constitute an immense class of compounds in number and diversity[1,2] and exhibit remarkable chemical and physical properties, their actual and potential applications spanning a variety of fields, including medicine, catalysis, solid-state technology, and chemical analysis.[2−4] The formation of polymeric oxoanions is, in general, a phenomenon largely limited to the transition metals of groups 5 and 6 and, in particular, to molybdenum and tungsten, which have been considered the "polyoxoanion formers par excellence".[2]

Most of the typical polyanion structures exhibit interpenetrating closed loops, formed by the metal centers and the bridging-oxygen atoms linking the octahedral units, that have been regarded as a type of macrocyclic bonding system.[5−9] Nomiya and Miwa[5] have proposed a connection between the structural stability of polyoxometalates and the number of closed loops per MO_6 octahedron in the form of an index (η) defined as

$$\eta = \frac{\Sigma BC}{A} \tag{1}$$

where A is the number of octahedra constituting the polyanion cage, B is the number of MO_6 units constituting the closed loop, and C is the number of closed loops. It should be noted that the polyanion cage is not necessarily identical with the whole structure, although it does comprise most of it.[5]

A large number of isopoly and heteropoly species have been analyzed,[5−9] and it has been concluded that the structural stability index can be related to various properties of the polyanion systems. A particularly important observation is that the larger the value of the index, the more a polyoxometalate appears to be stabilized. In addition to their (apparent) contribution to the stability of the polyanions, it

* To whom correspondence should be addressed. Telephone: +44 1482 466549. Fax: +44 1482 466410. E-mail: A.J.Bridgeman@hull.ac.uk.
† University of Hull.
‡ University of Cambridge.

(1) Pope, M. T. *Heteropoly and Isopoly Oxometalates*; Springer-Verlag: Heidelberg, Germany, 1983.
(2) Pope, M. T.; Müller, A. *Ang. Chem., Int. Ed. Engl.* **1991**, *30*, 34.
(3) Baker, L. C. W.; Glick, D. C. *Chem. Rev.* **1998**, *98*, 3.
(4) Pope, M. T., Müller, A., Eds. *Polyoxometalates: from Platonic Solids to Anti-retroviral Activity*; Kluwer: Dordrecht, The Netherlands, 1994.
(5) Nomiya, K.; Miwa, M. *Polyhedron* **1984**, *3*, 341.
(6) Nomiya, K.; Miwa, M. *Polyhedron* **1985**, *4*, 89.
(7) Nomiya, K.; Miwa, M. *Polyhedron* **1985**, *4*, 675.
(8) Nomiya, K.; Miwa, M. *Polyhedron* **1985**, *4*, 1407.
(9) Nomiya, K. *Polyhedron* **1987**, *6*, 309.

10.1021/ic011086f CCC: $22.00
Published on Web 03/07/2002

has been suggested[10] that closed loops may also play a significant role in electron-transfer processes, by providing pathways for electron delocalization, via π-bonding type interactions between metal d and bridging-oxygen p orbitals.

The structure of $[M_6O_{19}]^{n-}$ isopolyanions is characterized by the presence of one terminal M−O bond at each metal center, and thus, they belong to the type-I category in Pope's classification scheme.[1] Type-I systems can undergo reversible reactions, with minor structural changes. This redox behavior can in principle be understood in terms of the electronic structures of $[MOL_5]$ complexes, which are suitable models for the MO_6 units in the anionic clusters. In monooxo species, the lowest unoccupied molecular orbital (LUMO) is, to a first approximation, M d_{xy}-like and nonbonding. Therefore, the additional electrons introduced by reduction are not expected to cause significant structural disruption.

Although polyoxoanion chemistry is an extremely rich area of experimental research, high-level calculations on polyoxometalates have remained relatively scarce, mainly due to the intensive computational demands imposed by the large size of these species. Most of the first-principle studies—at the Hartree−Fock (HF) or density-functional (DF) levels of theory—have been carried out by Bénard, Poblet, and co-workers,[11−19] who have investigated a variety of systems and chemical phenomena, including the relative basicities of oxygen sites, redox properties, host−guest interactions, and inclusion complexes. Many of these calculations have primarily concentrated on the application of molecular electrostatic-potential distributions to understanding the chemical structures and interactions in the polyanion clusters and have recently been reviewed.[20] Borshch and co-workers have reported DF investigations dealing with electron delocalization[21,22] in substituted isopoly and heteropoly species and with the reducibility of Keggin anions.[23] In addition to the HF and DF research, several computational studies of the catalytic properties of Keggin anions[24−27] and an investigation of aromaticity in $[M_6O_{19}]^{n-}$ clusters[28] have been performed using the Xα method.

In this article we report the results of density-functional calculations on the oxidized $[Nb_6O_{19}]^{8-}$, $[Ta_6O_{19}]^{8-}$, $[Mo_6O_{19}]^{2-}$, and $[W_6O_{19}]^{2-}$ anions and on the one-electron- and two-electron-reduced forms of the Mo and W systems. The optimized molecular structures and a description of chemical bonding in terms of molecular-orbital, population, and bonding-energy analyses are presented, and a discussion of the nature and properties of closed-loop orbital interactions is included.

Computational Approach

All density-functional calculations reported in this work were performed with the ADF[29,30] program. Functionals based on the Vosko−Wilk−Nusair[31] (VWN) form of the local density approximation[32] (LDA) and on a combination (labeled BP86) of Becke's 1988 exchange[33] and Perdew's 1986 correlation[34] corrections to the LDA were employed. Slater-type-orbital (STO) basis sets (ADF type IV) of triple-ζ quality incorporating frozen cores and the ZORA relativistic approach[29,30] were utilized.

The functional and basis-set choices were based on the results of tests performed on several $[MO_4]$ and $[M_2O_7]$ species.[35,36] Geometry optimizations were carried out using LDA methods, whereas data on thermochemistry and energetics were extracted from single-point BP86 calculations. Bond and valency indexes were obtained according to the definitions proposed by Mayer[37,38] and by Evarestov and Veryazov,[39] with a program[40] designed for their calculation from the ADF output file. Graphics of molecular orbitals were generated with the MOLEKEL[41] program.

Results and Discussion

Molecular Structure. Calculated M−O bond distances for the oxidized anions and for the Mo and W one-electron- and two-electron-reduced systems are given in Table 1. A structural scheme showing atom labels is presented in Figure 1. Experimental results for the oxidized species are also

(10) King, R. B. *Inorg. Chem.* **1991**, *30*, 4437.
(11) Rohmer, M.-M.; Ernenwein, R.; Ulmschneider, M.; Wiest, R.; Bénard, M. *Int. J. Quantum Chem.* **1991**, *40*, 723.
(12) Kempf, J.-Y.; Rohmer, M.-M.; Poblet, J.-M.; Bo, C.; Bénard, M. *J. Am. Chem. Soc.* **1992**, *114*, 1136.
(13) Rohmer, M.-M.; Bénard, M. *J. Am. Chem. Soc.* **1994**, *116*, 6959.
(14) Devémy, J.; Rohmer, M.-M.; Bénard, M.; Ernenwein, R. *Int. J. Quantum Chem.* **1996**, *58*, 267.
(15) Rohmer, M.-M.; Devémy, J.; Wiest, R.; Bénard, M. *J. Am. Chem. Soc.* **1996**, *118*, 13007.
(16) Maestre, J. M.; Sarasa, J. P.; Bo, C.; Poblet, J. M. *Inorg. Chem.* **1998**, *37*, 3071.
(17) Maestre, J. M.; Poblet, J. M.; Bo, C.; Casañ-Pastor, N.; Gomez-Romero, P. *Inorg. Chem.* **1998**, *37*, 3444.
(18) Dolbecq, A.; Guirauden, A.; Fourmigué, M.; Boubekeur, K.; Batail, P.; Rohmer, M.-M.; Bénard, M.; Coulon, C.; Sallé, M.; Blanchard, P. *J. Chem. Soc., Dalton Trans.* **1999**, 1241.
(19) Maestre, J. M.; López, X.; Bo, C.; Poblet, J. M.; Casañ-Pastor, N. *J. Am. Chem. Soc.* **2001**, *123*, 3749.
(20) Rohmer, M.-M.; Bénard, M.; Blaudeau, J.-P.; Maestre, J.-M.; Poblet, J.-M. *Coord. Chem. Rev.* **1998**, *178−180*, 1019.
(21) Duclusaud, H.; Borshch, S. A. *Inorg. Chem.* **1999**, *38*, 3489.
(22) Duclusaud, H.; Borshch, S. A. *J. Am. Chem. Soc.* **2001**, *123*, 2825.
(23) Borshch, S. A.; Duclusaud, H.; Millet, J. M. M. *Appl. Catal., A* **2000**, *200*, 103.
(24) Eguchi, K.; Seiyama, T.; Yamazoe, N.; Katsuki, S.; Taketa, H. *J. Catal.* **1988**, *111*, 336.
(25) Taketa, H.; Katsuki, S.; Eguchi, K.; Seiyama, T.; Yamazoe, N. *J. Phys. Chem.* **1986**, *90*, 2959.
(26) Xiao, S. X.; Ji, J.; Chen, T. L.; Cai, T. X.; Yan, G. S. *THEOCHEM* **1990**, *63*, 33.
(27) Chen, T. L.; Ji, J.; Xiao, S. X.; Cai, T. X.; Yan, G. S. *Int. J. Quantum Chem.* **1992**, *44*, 1015.
(28) Cai, T.; Chen, Z. D.; Wang, X. Z.; Li, L. M.; Lu, J. X. *Prog. Nat. Sci.* **1997**, *7*, 554.
(29) ADF2000.02: Baerends, E. J.; Ellis, D. E.; Ros, P. *Chem. Phys.* **1973**, *2*, 41. Versluis, L.; Ziegler, T. *J. Chem. Phys.* **1988**, *322*, 88. teVelde, G.; Baerends, E. J. *J. Comput. Phys.* **1992**, *99*, 84. FonsecaGuerra, G.; Snijders, J. G.; teVelde, G.; Baerends, E. J. *Theor. Chem. Acc.* **1998**, *99*, 391.
(30) te Velde, G.; Bickelhaupt, F. M.; Baerends, E. J.; FonsecaGuerra, C.; van Gisbergen, S. J. A.; Snijders, J. G.; Ziegler, T. *J. Comput. Chem.* **2001**, *22*, 931.
(31) Vosko, S. H.; Wilk, L.; Nusair, M. *Can. J. Phys.* **1980**, *58*, 1200.
(32) Kohn, W.; Sham, L. J. *Phys. Rev.* **1965**, *140*, A1133.
(33) Becke, A. D. *Phys. Rev. A* **1988**, *38*, 3098.
(34) Perdew, J. P. *Phys. Rev. B* **1986**, *33*, 8822.
(35) Bridgeman, A. J.; Cavigliasso, G. *Polyhedron* **2001**, *20*, 2269.
(36) Bridgeman, A. J.; Cavigliasso, G., *J. Phys. Chem. A* **2001**, *105*, 7111.
(37) Mayer, I. *Chem. Phys. Lett.* **1983**, *97*, 270.
(38) Mayer, I. *Int. J. Quantum Chem.* **1984**, *26*, 151.
(39) Evarestov, R. A.; Veryazov, V. A. *Theor. Chim. Acta* **1991**, *81*, 95.
(40) MAYER. A program to calculate Mayer bond-order indexes from the output of the electronic structure packages GAMESS-UK, GAUSSIAN, and ADF, written by A. J.Bridgeman, University of Hull, 2001. Available from the author on request.
(41) MOLEKEL: An Interactive Molecular Graphics Tool: Portmann S.; Lüthi, H. P. *Chimia* **2000**, *54*, 766.

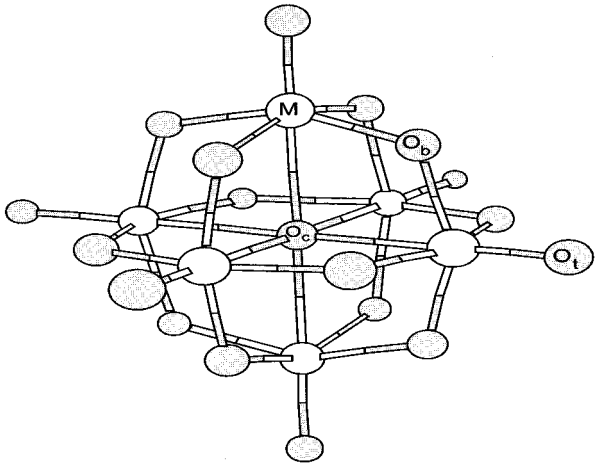

Figure 1. Structural and atom-labeling scheme for $[M_6O_{19}]^{n-}$ anions.

Table 1. M−O Bond Distances (in pm) for Oxidized Anions and Mo and W Reduced Anions with Available Experimental Results in Parentheses

molecule	M−O_c	M−O_b	M−O_t
$[Nb_6O_{19}]^{8-}$	244 (238)	201 (201)	188 (177)
$[Ta_6O_{19}]^{8-}$	244 (238)	202 (199)	190 (180)
$[Mo_6O_{19}]^{2-}$	232 (232)	193 (192)	171 (168)
$[Mo_6O_{19}]^{3-}$	233	193	173
$[Mo_6O_{19}]^{4-}$	234	194	174
$[W_6O_{19}]^{2-}$	234 (233)	194 (192)	173 (169)
$[W_6O_{19}]^{3-}$	235	195	175
$[W_6O_{19}]^{4-}$	237	196	176

included. These were taken from the compilations of Tytko and co-workers[42] and correspond to O_h-symmetry averages of bond-length values observed in crystalline phases. Computational data for reduced anions are limited to Mo and W because the considerably high negative charge of the Nb and Ta clusters causes difficulties in handling virtual orbitals.

For $[Nb_6O_{19}]^{8-}$ and $[Ta_6O_{19}]^{8-}$, bridging-bond (M−O_b) distances compare well with experimental results, but the calculated lengths of central (M−O_c) and, especially, terminal (M−O_t) bonds are significantly longer than the average values in the crystal structures. The overall agreement between calculation and experiment improves considerably for $[Mo_6O_{19}]^{2-}$ and $[W_6O_{19}]^{2-}$, including M−O_t distances, although these are the parameters showing the greatest discrepancies.

Recent investigations on several oxoanions[35] have shown that, despite corresponding to gas-phase systems and therefore lacking solid-state effects, isolated-molecule calculations (as those reported in this work) are able to satisfactorily reproduce experimental condensed-phase information. In cases where significant deviations are observed, a high negative charge appears to be an important factor (for example, the computational−experimental accord is appreciably better for $[SO_4]^{2-}$ and $[CrO_4]^{2-}$ than it is for $[SiO_4]^{4-}$ and $[TiO_4]^{4-}$, respectively). This negative-charge influence is, therefore, also likely to be affecting the present results for the Nb and Ta anions.

The products obtained by reducing type-I polyoxometalates are known to retain the general structural features of the

(42) Tytko, K. H.; Mehmke, J.; Fischer, S. *Struct. Bonding* **1999**, *93*, 129.

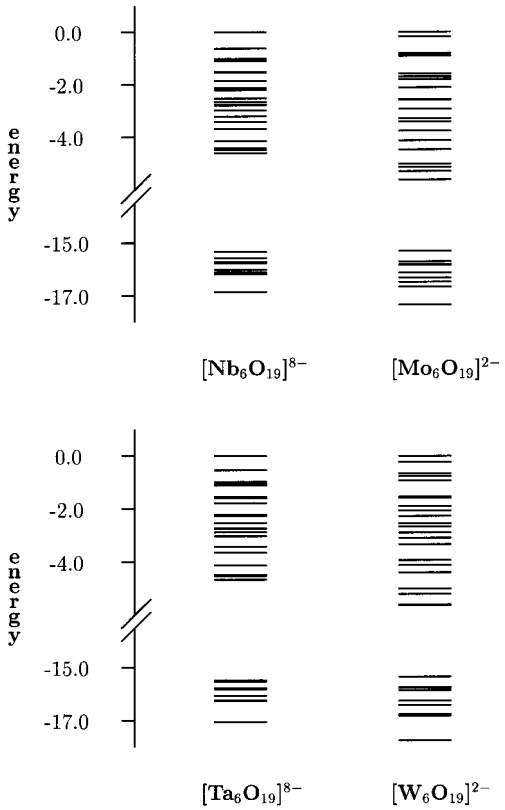

Figure 2. Eigenvalue (in eV) diagram for occupied valence levels of oxidized anions.

oxidized clusters.[1−3] This is observed in the results of the calculations on Mo and W reduced anions. Only a small lengthening of the M−O distances (about 1−2 pm in each reduction step) occurs, and minimal changes to the global octahedral arrangement have been detected, even when the molecular symmetry had been lowered to allow for the possibility of geometry variations.

Electronic Structure. Eigenvalue diagrams for the occupied valence levels of the oxidized anions are given in Figure 2. A comparison of absolute orbital eigenvalues is not possible due to the differences in the total charge of the species. Therefore, molecular-orbital energies are given relative to a value of 0.0 eV assigned to the $4t_{1g}$ orbitals. These constitute the highest-occupied level (HOMO) and possess, almost exclusively, bridging-oxygen p character, in all four species.

Qualitative descriptions are presented in Figure 3 and Table 2. Figure 3 shows the predominant metal and oxygen contributions to the valence molecular orbitals, whereas Table 2 contains some details of the composition of M−O bonding interactions. These schemes are entirely qualitative, and no accurate quantitative correlation exists among the positions of the atomic and molecular energy levels. They are intended to summarize the most general and representative characteristics of the electronic structure of the polyanions by highlighting the major atomic contributions to the molecular orbitals.

(a) Molecular Orbital Schemes. The molecular orbital diagrams of all $[M_6O_{19}]^{n-}$ anions are characterized by the presence of two distinct sets of molecular energy levels,

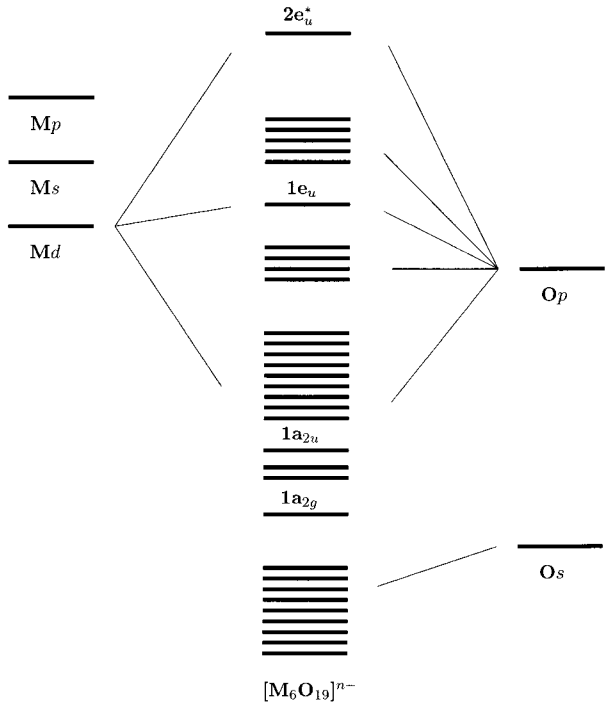

Figure 3. Qualitative molecular orbital diagram showing predominant metal and oxygen contributions to the valence levels of oxidized anions.

Table 2. Symmetry Decomposition of Molecular Orbitals Possessing Substantial Metal-d and Oxygen-p Character

symmetry species	bonding properties
t_{1u}	M−O_c, M−O_b, M−O_t
a_{1g}, e_g, t_{2g}, t_{2u}	M−O_b, M−O_t
a_{2g}, a_{2u}, e_u	M−O_b
t_{1g}	M−O_t

separated by a gap of approximately 10 eV. The low-lying orbitals comprise a predominantly O s (O_c, O_b, O_t) and nonbonding band. The high-lying set can be divided into two additional bands. Most higher energy levels correspond to nonbonding combinations of p-type functions from O_c, O_b, and O_t atoms, whereas most lower-energy levels are composed of orbitals that incorporate significant contributions from both the metal and oxygen atoms and represent M−O bonding interactions of largely M d−O p character. The $1e_u$ orbitals appear as a distinctive level in that, despite being M−O bonding, they lie considerably higher than the rest of the M d−O p molecular orbitals and split the O p-based band.

The predominant contributions of the different types of oxygen atoms to M−O bonding are described by the symmetry-based decomposition of the levels in the M d−O p band, shown in Table 2. In addition, the lowest unoccupied level (LUMO) is particularly important as it is the acceptor of the additional electrons in the reduced species. The LUMO corresponds to the $2e_u$ level (Figure 3) and is characterized by participation of metal d (∼0.55−0.60) and, exclusively, bridging-oxygen p (∼0.40−0.45) orbitals.

A three-dimensional spatial representation of the two orbitals comprising the $2e_u$ level is given in Figure 4. The first symmetry-adapted combination (part a) involves 4 of the 6 metal centers and 8 of the 12 bridging-oxygen atoms, whereas the second symmetrized orbital (part b) incorporates

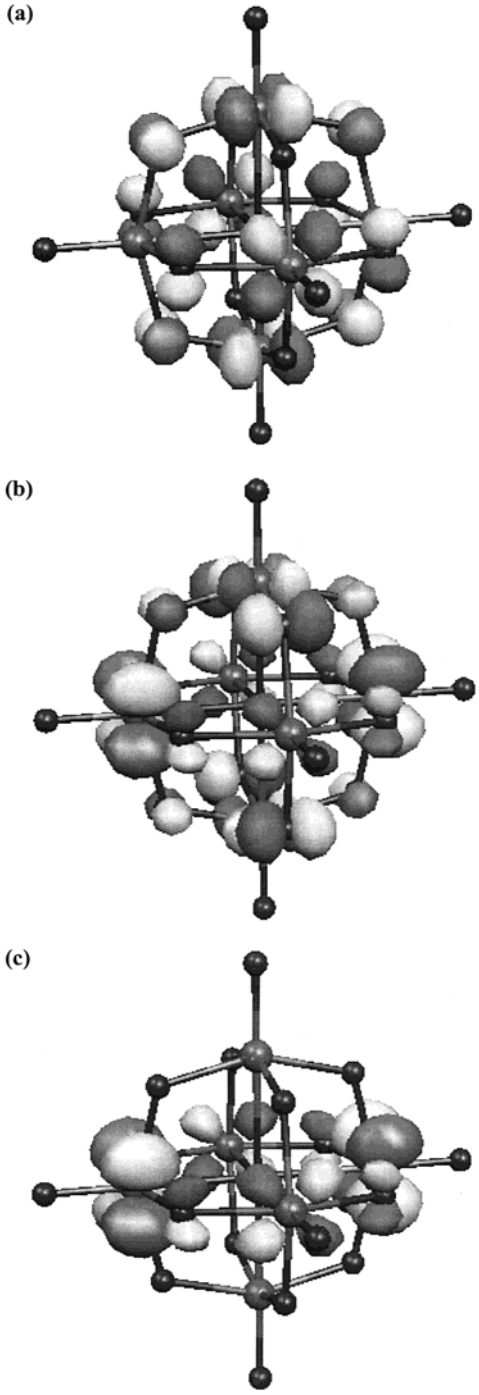

Figure 4. Spatial representation of the $2e_u$ orbitals: (a, b) three-dimensional structure; (c) $[M_4O_4]$ closed loops.

all of the M and O_b sites and can also be described in terms of 3 planar $[M_4O_4]$ rings, the closed loops proposed by Nomiya and Miwa.[5] The orbital properties of these rings are shown in the spatial representation of the $2e_u$ closed loops, given in Figure 4 (part c). They correspond to π interactions between metal d_{xy}-like and bridging-oxygen p orbitals and can be viewed as extensively delocalized analogues of the $2b_2$ orbital in the model monooxo complexes,[43] shown in Figure 5.

(43) Bridgeman, A. J.; Cavigliasso, G. *J. Chem. Soc., Dalton Trans.* **2001**, 3556.

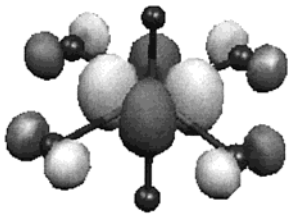

Figure 5. Spatial representation of the LUMO in $[MOCl_5]^{n-}$ complexes.

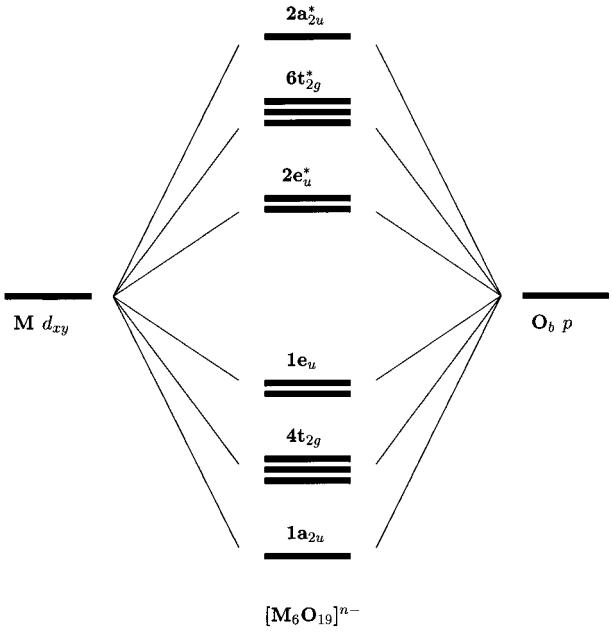

Figure 6. Qualitative molecular orbital diagram showing orbital interactions of M d_{xy}-like and O_b character.

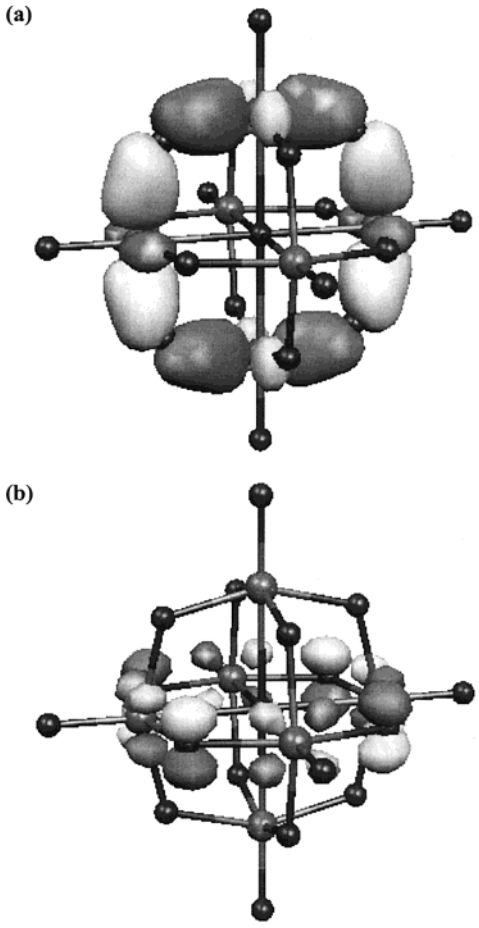

Figure 7. Spatial representation of bonding $[M_4O_4]$ closed loops: (a) a_{2g} orbital; (b) a_{2u} orbital.

These results are partially in agreement with the analysis presented by King,[10] who has considered the idea that electron delocalization in $[M_6O_{19}]^{n-}$ anions may be realized through M−O−M bridges and has suggested, on the basis of topological models, that overlap of metal d_{xy} orbitals would create a bonding LUMO. However, Figure 4 and the overlap-population data (−0.1216 for Mo and −0.1285 for W) indicate that the $2e_u$ orbitals are M−O_b antibonding. This discrepancy arises as a consequence of assuming that the LUMO in the individual MO_6 units is a nonbonding M d_{xy} orbital.[10] In contrast, calculations on model $[MOL_5]$ complexes[43] have revealed antibonding interactions between the metal atom and the equatorial ligands in the corresponding LUMOs (Figure 5), analogous to those observed in the polynuclear systems.

In the $[M_6O_{19}]^{n-}$ anions, interactions predominantly involving M d_{xy}-like and O_b orbitals span the a_{2u}, e_u, and t_{2g} species. The qualitative scheme in Figure 6 shows that these interactions generate six occupied M−O_b bonding ($1a_{2u}$, $4t_{2g}$, $1e_u$) and six vacant M−O_b antibonding ($2e_u$, $6t_{2g}$, $2a_{2u}$) molecular orbitals. King's topological analysis[10] yields an exactly reverse ordering for the latter and, thus, a nondegenerate LUMO instead of the $2e_u$ level.

(b) Closed Loops and Bonding. It has been pointed in the Introduction that Nomiya and Miwa have developed the idea—and quantified it through the index defined by eq 1—of the importance of metal−oxygen interactions along M−O_b closed loops as a structural-stability factor in polyoxometalates. These authors have also suggested that both σ and π bonding between the metal and bridging-oxygen atoms should be involved.[5]

The analysis in Table 2 indicates that three groups of levels ($1a_{2g}$, $1a_{2u}$, $1e_u$) involve M−O bonding molecular orbitals containing contributions exclusively (because of symmetry constraints) from bridging-oxygen atoms. As in the case of the (vacant and antibonding) $2e_u$ level, these three orbitals are characterized by three-dimensional electron-density distributions but can also be described in terms of planar $[M_4O_4]$ rings. Figure 7 gives a spatial representation of $1a_{2g}$ and $1a_{2u}$ closed loops. The $1e_u$ orbitals represent the bonding counterpart of the $2e_u$ level, which is shown in Figure 4.

The interactions along the closed loops are of both σ ($1a_{2g}$) and π ($1a_{2u}$, $1e_u$) character, as suggested by Nomiya and Miwa. Their corresponding relative contributions to the bonding energy (E_B) of the polyanions can be quantitatively characterized by decomposition of E_B according to

$$E_B = E_O + E_P + E_E \qquad (2)$$

and subsequent analysis of the components of E_O. In eq 2, E_O, E_P, and E_E are respectively orbital-mixing, Pauli-repulsion, and electrostatic-interaction terms. Descriptions of the physical significance of these properties have been

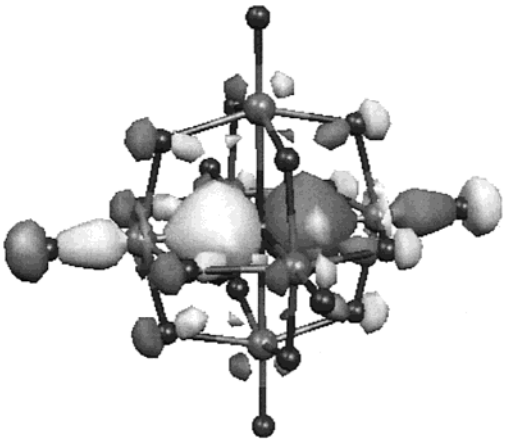

Figure 8. Spatial representation of the $6t_{1u}$ orbitals.

Table 3. Orbital-Interaction Energies (in eV) for Oxidized Anions

molecule	a_{2g}	a_{2u}	e_u	t_{1u}	total
$[Nb_6O_{19}]^{8-}$	−15.37	−11.02	−11.52	−109.80	−396.77
$[Ta_6O_{19}]^{8-}$	−13.85	−9.58	−8.53	−135.93	−419.78
$[Mo_6O_{19}]^{2-}$	−14.75	−9.39	−6.95	−168.33	−505.88
$[W_6O_{19}]^{2-}$	−15.94	−10.35	−8.84	−181.54	−549.46

given by Landrum, Goldberg, and Hoffmann[44] and by Baerends and co-workers.[30] Both E_O and E_P represent orbital-interaction effects, but the former is stabilizing whereas the latter is destabilizing. The E_E contribution is primarily dominated by the nucleus−electron attractions and, therefore, has a stabilizing influence.

Interaction energies for a_{2g}, a_{2u}, and e_u orbitals and total E_O values for the four oxidized isopolyanions are given in Table 3. The t_{1u} orbitals are also included for comparison, as they contain all types of oxygen sites (Table 2 and Figure 8) and are the largest component of the E_O term. The contributions from the exclusively M−O_b group are important, but they represent 6−10% of the total E_O energy and are three to six times smaller than that from the t_{1u} orbitals. Furthermore, the a_{1g}, e_g, t_{2g}, and t_{2u} terms, all including M−O_t bonding (Table 2), are also greater than the a_{2g}, a_{2u}, and e_u energies. These results suggest that the closed-loop mode of orbital mixing does not stand out as a stabilizing factor.

(c) Reduced Anions. The added electrons in the reduced anions are normally considered to be "delocalized according to various time scales over certain atoms or regions of the structures".[3] Two mechanisms have been proposed to explain these electron-delocalization phenomena: thermally activated hopping and ground-state delocalization presumably through π-bonding-type interactions between metal d and bridging-oxygen p orbitals.

Experimental results for the $[Mo_6O_{19}]^{3-}$ cluster, including electron-spin-resonance (ESR)[45] and ^{17}O nuclear magnetic resonance (NMR)[46] data, have been reported. The ESR studies have indicated that the ground state of this one-electron-reduced system is orbitally nondegenerate and have suggested that the ground-state delocalization seems to be restricted to ligand O atoms without involving neighboring Mo sites and that it appears to be of relatively small magnitude. From the NMR information it has been pointed out that the additional electron is delocalized over all the metal atoms in the anion (on the NMR time scale), which possesses effective cubic symmetry.

Table 4. Comparison of M−O Bond Distances (in pm) for C_{4v} and O_h Forms of Mo and W One-Electron Reduced Anions

		C_{4v}		
molecule	parameter	$^2A_2$	$^2B_2$	O_h
$[Mo_6O_{19}]^{3-}$	M−O_c	232.8−233.6	232.4−233.4	233.0
	M−O_b	192.3−195.1	191.6−194.4	193.3
	M−O_t	172.6−172.8	172.5−172.7	172.5
$[W_6O_{19}]^{3-}$	M−O_c	235.0−235.9	234.4−235.7	235.2
	M−O_b	193.4−196.7	192.1−195.7	194.5
	M−O_t	173.7−174.7	173.6−174.8	174.6

Table 5. Bonding-Energy Analysis (in eV) for Mo and W Two-Electron-Reduced Anions (S, Singlet; T, Triplet)

molecule	state	E_O	E_E	E_P	E_B
$[Mo_6O_{19}]^{4-}$	T	−477.15	−161.37	+442.51	−196.01
	S	−477.01	−161.40	+442.58	−195.83
$[W_6O_{19}]^{4-}$	T	−515.47	−189.79	+504.40	−200.85
	S	−515.50	−189.91	+504.74	−200.67

The fact that the LUMO in the oxidized anions is an e_u level leads to an orbitally degenerate ground state for the one-electron-reduced anions in calculations that utilize O_h molecular symmetry. The possibility of observing distortions that would remove the degeneracy and could also allow for electron localization has been explored by lowering the symmetry to C_{4v}. As mentioned in the Molecular Structure section, only minimal geometrical changes are observed, and the octahedral arrangement is largely retained in the reduced anions. The $2e_u$ level is split into $6a_2$ and $8b_2$ orbitals (C_{4v}) and, thus, the degeneracy is effectively removed, but the energy differences between these two orbitals and the corresponding electronic states, $^2A_2$ and $^2B_2$, are negligible and no localization has been detected.

Table 4 summarizes the structural data for the C_{4v} and O_h forms. The $6a_2$ and $8b_2$ orbitals in the former are respectively equivalent to the symmetrized functions in parts (a) and (b) of Figure 4 and accommodate the unpaired electron in the $^2A_2$ and $^2B_2$ states, leading to a slight elongation and compression along the z axis. The individual geometrical parameters and the general configuration of the O_h species are averages of the two C_{4v} states, thus resembling a dynamic Jahn−Teller effect. It can be concluded that the calculations on the $[Mo_6O_{19}]^{3-}$ anion suggest that the additional electron is delocalized over the whole $[MO_b]$ network and, therefore, agree with the ^{17}O NMR results.

Calculations on the Mo and W $[M_6O_{19}]^{4-}$ anions were performed for the singlet (S) and triplet (T) states, and the results are given in Table 5 in the form of the bonding-energy analysis of eq 2. The S and T states are found to be of similar bonding stability, and their respective orbital, Pauli, and electrostatic terms do not show significant differences. Additional calculations were carried out using the C_{4v}

(44) Landrum, G. A.; Goldberg, N.; Hoffmann, R. *J. Chem. Soc., Dalton Trans.* **1997**, 3605.

(45) Sanchez, C.; Livage, J.; Launay, J. P.; Fournier, M.; Jeannin, Y. *J. Am. Chem. Soc.* **1982**, *104*, 3194.

(46) Piepgrass, K.; Barrows, J. N.; Pope, M. T. *J. Chem. Soc., Chem. Commun.* **1989**, 10.

arrangement and an unrestricted broken-symmetry molecular-orbital formalism. As observed in the one-electron-reduced systems, no appreciable changes to the structural, electronic, and thermochemical properties of the $[M_6O_{19}]^{4-}$ species have been found, for any of the four—$(6a_2)^2$, $(8b_2)^2$, paired $(6a_2)^1$ $(8b_2)^1$, and unpaired $(6a_2)^1$ $(8b_2)^1$—configurations explored.

The present computational results agree satisfactorily with experimental evidence indicating absence of important structural changes after reduction of type-I polyoxometalates has taken place. The explanation lies in that the effect of the orbitals occupied by the added electrons on the stability of the clusters is rather limited (Table 3), despite their formally antibonding character. As noted in the Molecular Orbital Schemes section, this argument is different from that proposed by King.[10]

(d) Comparison to Natural-Bond-Orbital Results. Cai and co-workers[28] have reported a natural-bond-orbital (NBO) analysis of the electronic structure of $[M_6O_{19}]^{n-}$ anions, with emphasis on the aromatic properties of these clusters. The origin of the aromaticity has been associated with conjugated M−O_b d−p π bonding along the eight-membered $[M_4O_4]$ rings. The description of these metal−oxygen interactions involves in-plane and out-of-plane delocalization, the latter being significantly more important.

The results of our calculations are in general agreement with the NBO analysis. The e_u and a_{2u} closed loops in Figures 4c and 7b, respectively, are examples of out-of-plane interactions, whereas the spatial representation of the $3t_{2g}$ orbital, given in Figure 9, corresponds to in-plane π-like delocalization (the $3t_{2g}$ level has not been included in the scheme of Figure 6 because, as shown by Figure 9, it exhibits considerable M−O_t, in addition to M−O_b, character). Electron delocalization in polyoxometalates has frequently been compared[10,28] to analogous properties of typical aromatic systems such as hydrocarbon rings and boranes. It is interesting to note that in-plane and out-of-plane modes of bonding have also been suggested for P−N interactions in cyclophosphazenes.[47,48]

A difference from the NBO study is worthy of comment. Cai and co-workers have described the M−O_c interactions in terms of M−O_c−M bonds analogous to those involving the $6t_{1u}$ orbitals (Figure 8), but they have also considered that an M_6-to-O_c bond is formed between the central-oxygen s orbital and an a_{1g} combination of metal p functions. However, as mentioned in the molecular-orbital description, our results indicate that, to a large extent, all O s orbitals occur in low-lying nonbonding levels and that Mp orbitals are almost entirely unpopulated (Table 6). Consequently, M p−O s interactions do not appear to contribute to bonding in the $[M_6O_{19}]^{n-}$ polyanions.

Population Methods. The results presented in this section are based on Mulliken and Mayer methodology. These methods are known to exhibit basis-set dependence, but (relative) Mulliken charges and Mayer bond indexes can nonetheless provide valuable chemical information for inorganic systems, if uniformity and consistency of the basis sets are maintained.[49] Furthermore, Mulliken analysis has been described as "not an arbitrary choice . . . but consistent with the internal structure of the molecular-orbital formalism".[37]

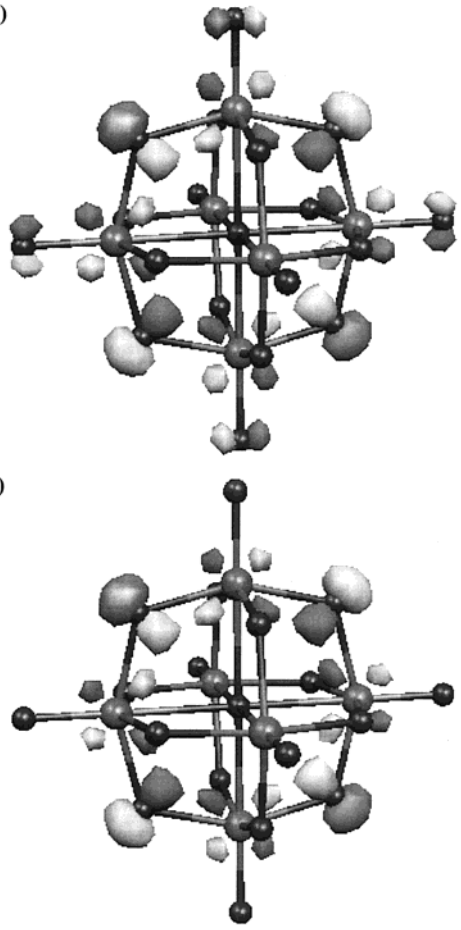

Figure 9. Spatial representation of $3t_{2g}$ orbitals: (a) three-dimensional structure; (b) $[M_4O_4]$ closed loops.

Table 6. Mulliken Charges and Metal Orbital Populations for Oxidized Anions and Mo and W Reduced Anions

	charges				M orbitals		
molecule	M	O_c	O_b	O_t	s	p	d
$[Nb_6O_{19}]^{8-}$	1.58	−0.98	−0.92	−0.91	0.19	0.00	3.29
$[Ta_6O_{19}]^{8-}$	1.72	−1.07	−0.94	−0.99	0.27	0.08	2.93
$[Mo_6O_{19}]^{2-}$	2.19	−1.19	−0.83	−0.66	0.00	0.17	3.80
$[Mo_6O_{19}]^{3-}$	2.11	−1.18	−0.85	−0.72	0.00	0.17	3.86
$[Mo_6O_{19}]^{4-}$	2.02	−1.17	−0.86	−0.77	0.00	0.16	3.93
$[W_6O_{19}]^{2-}$	2.30	−1.16	−0.87	−0.71	0.10	0.16	3.44
$[W_6O_{19}]^{3-}$	2.22	−1.16	−0.88	−0.77	0.11	0.16	3.51
$[W_6O_{19}]^{4-}$	2.14	−1.15	−0.90	−0.82	0.13	0.15	3.58

(a) Mulliken Analysis. Mulliken charges for all atoms and metal basis-function populations are given in Table 6. The results for the oxidized systems correspond to metal d^3−d^4 electronic configurations, in contrast to the formal d^0 assignment, and the charges are considerably smaller than the formal oxidation states. The s and p orbitals are sparingly populated, in accordance with the molecular orbital analysis

(47) Greenwood, N. N.; Earnshaw, A. *Chemistry of the Elements*, 2nd ed.; Butterworth-Heinemann: Boston, MA, 1997.
(48) Huheey, J. E.; Keiter, E. A.; Keiter, R. L. *Inorganic Chemistry*, 4th ed.; Harper Collins: New York, 1993.
(49) Bridgeman, A. J.; Cavigliasso, G., Ireland, L. R.; Rothery, J. *J. Chem. Soc., Dalton Trans.* **2001**, 2095.

Table 7. Mayer Indexes for Oxidized Anions (Results from Classical Bond-Valence Analysis in Parentheses) and Mo and W Reduced Anions

molecule	M−O_c	M−O_b	M−O_t
$[Nb_6O_{19}]^{8-}$	0.30 (0.25)	0.77 (0.78)	1.51 (1.10)
$[Ta_6O_{19}]^{8-}$	0.25 (0.25)	0.77 (0.76)	1.53 (1.06)
$[Mo_6O_{19}]^{2-}$	0.19 (0.38)	0.75 (0.96)	1.68 (1.64)
$[Mo_6O_{19}]^{3-}$	0.20	0.74	1.64
$[Mo_6O_{19}]^{4-}$	0.21	0.74	1.59
$[W_6O_{19}]^{2-}$	0.18 (0.36)	0.77 (0.94)	1.73 (1.57)
$[W_6O_{19}]^{3-}$	0.19	0.76	1.68
$[W_6O_{19}]^{4-}$	0.19	0.75	1.63

indicating almost exclusive participation of M d functions in M−O bonds. The slightly higher s and lower d characters of Ta and W configurations, with respect to those of Nb and Mo, are probably a consequence of the stronger relativistic effects in the 5d elements.[50] These characteristics have also been observed in the $[MO_4]^{n-}$ and $[M_2O_7]^{n-}$ anions[35,36] and $[MOCl_5]^{n-}$ complexes.[43]

The O values reveal that the negative charge is distributed over all types of atoms and that the excess charge in the Nb and Ta anions, and in the reduced species, is accepted by the surface sites, especially the terminal O centers. These observations are similar to those made by Tytko and co-workers from results based on a bond-valence model for polyoxometalates.[42,51] These authors have also considered that the description of the $[M_6O_{19}]^{2-}$ anions as a neutral $[M_6O_{18}]$ cage encapsulating an oxide ion[52] is incorrect. This point is discussed further in the next sections.

The geometrical modifications of the reduced anions seem to be substantially driven by stronger repulsions involving external oxygen atoms, in particular the terminal sites as these display the largest charge increase. The changes in the Mulliken populations caused by each one-electron reduction step correspond to a partition of the excess unit charge in approximately 0.34 (O_t):0.18 (O_b):0.48 (M) proportions. This result reflects the delocalization mechanism associated with the M−O_b π-like orbitals that accept the additional electrons and the increased ionicity of the M−O_t bonds.

(b) Bond-Order Analysis. Mayer bond-order indexes are given in Table 7. For the oxidized anions, additional results have been obtained with a bond-valence model based on the following relationship:[42]

$$\log s = \frac{d_0 - d}{B} \qquad (3)$$

Here s is the bond valence, d_0 is the single-bond length, B defines the slope of the bond length−bond valence functions, and d is a calculated bond distance.

Most of the computational indexes compare well with the bond-valence values. The differences are similar in magnitude to those observed in previous studies of oxoanions,[35,36] typically 0.2−0.3 units, with the exception of the results for the terminal bonds in the Nb and Ta systems. In these cases, the reasons for the greater discrepancy are the considerably longer optimized than experimental M−O distances (Table 1) and the fact that the Nb−O and Ta−O single-bond lengths in eq 3 are probably shorter than the predictions according to Mayer's definition would be.

Table 8. Bond Parameters for Equatorial M-Cl Groups in $[MOCl_5]^{n-}$ Complexes (M−Cl Bond Lengths in pm)

molecule	bond length	bond order
$[MoOCl_5]^-$	235	0.91
$[MoOCl_5]^{2-}$	242	0.66
$[MoOCl_5]^{3-}$	255	0.44
$[WOCl_5]^-$	235	0.96
$[WOCl_5]^{2-}$	242	0.68
$[WOCl_5]^{3-}$	252	0.47

The M−O_t distances in $[Nb_6O_{19}]^{8-}$ and $[Ta_6O_{19}]^{8-}$ are appreciably longer than those calculated for the model complexes,[43] $[MOCl_5]^{2-}$, but similar to those obtained for the four-coordinate $[MO_4]^{3-}$ and $[M_2O_7]^{4-}$ systems.[35,36] In these anions, as in the hexanuclear clusters, multiple-bonding character is predicted for the M−O_t interactions by both the Mayer and the molecular-orbital analyses of the electronic structure.

For all oxidized anions, the Mayer indexes reflect the trends in the M−O distances and reveal weak M−O_c bonds, approximately single character for M−O_b bonds, and significant, but as previously observed,[42] not maximized M−O_t multiple bonding. The differences found in the Nb and Ta systems with respect to the Mo and W species are primarily related to ionicity. The terminal bonds in the former and the central bonds in the latter are somewhat more ionic and exhibit smaller index values.

For the reduced Mo and W anions, the largest changes occur in the M−O_t bonds, the smaller indexes being associated with increased ionicity. The M−O_b bonds are only slightly affected by the additional electrons occupying the M−O_b antibonding levels. This is consistent with the $2e_u$ orbitals (or the equivalent $6a_2$ and $8b_2$ orbitals in the C_{4v} forms) representing relatively weak interactions that make comparatively small contributions to the bonding stability of the polyanions (Table 3). It is interesting to note that this result differs significantly from the redox behavior of the model Mo and W $[MOCl_5]^{n-}$ complexes,[43] in which a considerable lengthening of the equatorial bonds is caused by reduction (Table 8), and supports the idea (proposed by Nomiya and Miwa[5]) that the whole polyanion cage, and not only the properties of the individual MO_6 octahedra, should play an important role in electron-transfer phenomena.

A decomposition analysis of the bond indexes that utilizes the C_{4v} symmetry of the MO_6 unit is presented in Table 9. The σ or π nature of the M−O interactions is described respectively by an a_1 or e index for axial ligands and by an $a_1 + b_1$ or $b_2 + e$ index for equatorial ligands. The M−O_c bonds are largely σ-like, as also shown by Figure 8. The results given in Table 2 and the spatial plots of Figures 4, 7, and 9 indicate that the M−O_b interactions possess the typical molecular orbital structure of a multiple bond, with both σ and π contributions being important, and this feature is also present in the partial-index values in Table 9. The fact that the M−O_b distances and total-index values are, however, characteristic of an approximately single bond reflects the

(50) Kaltsoyannis, N. *J. Chem. Soc., Dalton Trans.* **1997**, 1.
(51) Tytko, K. H. *Struct. Bonding* **1999**, *93*, 67.
(52) Day, V. W.; Klemperer, W. G. *Science* **1985**, *228*, 533.

Table 9. Mayer-Index Decomposition (C_{4v} Symmetry) for M−O Bonds in Oxidized Anions

		decomposition	
molecule	M−O_c	a_1	e
$[Nb_6O_{19}]^{8-}$	0.30	0.30	0.00
$[Ta_6O_{19}]^{8-}$	0.25	0.25	0.00
$[Mo_6O_{19}]^{2-}$	0.19	0.14	0.05
$[W_6O_{19}]^{2-}$	0.18	0.16	0.02

		decomposition	
molecule	M−O_b	$a_1 + b_1$	$b_2 + e$
$[Nb_6O_{19}]^{8-}$	0.77	0.32	0.45
$[Ta_6O_{19}]^{8-}$	0.77	0.36	0.41
$[Mo_6O_{19}]^{2-}$	0.75	0.28	0.47
$[W_6O_{19}]^{2-}$	0.77	0.34	0.43

		decomposition	
molecule	M−O_t	a_1	e
$[Nb_6O_{19}]^{8-}$	1.51	0.66	0.85
$[Ta_6O_{19}]^{8-}$	1.53	0.66	0.87
$[Mo_6O_{19}]^{2-}$	1.68	0.58	1.10
$[W_6O_{19}]^{2-}$	1.73	0.63	1.10

Table 10. Covalency and Full-Valency Indexes for Oxygen Atoms in Oxidized Anions

	covalency			full valency		
molecule	O_c	O_b	O_t	O_c	O_b	O_t
$[Nb_6O_{19}]^{8-}$	1.94	1.79	1.81	2.35	2.18	2.19
$[Ta_6O_{19}]^{8-}$	1.65	1.75	1.73	2.17	2.17	2.17
$[Mo_6O_{19}]^{2-}$	1.41	1.92	2.10	2.08	2.23	2.30
$[W_6O_{19}]^{2-}$	1.31	1.88	2.08	1.99	2.21	2.30

effect of the extensive electron-density delocalization over the [M−O_b] network. The smaller bond orders for the M−O_t interactions in the Nb and Ta anions, compared with the Mo and W clusters, correspond to weaker π contributions, probably as a consequence of these being more directly affected by the much higher molecular charge.

(c) Oxygen Valency. Covalency and full-valency indexes for the oxygen atoms are shown in Table 10. The former are calculated as a sum of all Mayer indexes for a particular atom (and therefore include some contributions—for example O−O interactions—that may be small but not necessarily negligible), whereas the latter are a combined measure of covalent (covalency) and ionic (electrovalency) bonding on the basis of the Mayer and Mulliken results.

The weakness of internal (M−O_c) bonds in polyanions has been frequently ascribed to the trans influence of the strong M−O_t interactions.[1,2] This effect is evident in the values of distances and orders for individual central bonds in the $[M_6O_{19}]^{n-}$ anions. However, Tytko and co-workers [42] have pointed out that although the individual trans-to-oxo M−O bonds are longest and weakest, the O atoms involved interact with a high number of metal centers and may be as (or even more) strongly bound overall as the terminal-oxo ligands are. The results in Table 10 support this idea. In each species, the full-valency indexes for the various types of oxygen atoms are all rather similar, and the differences in the covalency values are much smaller than those observed for the individual bond orders.

There is a comparable trans-influence correlation in the covalency indexes to that observed between M−O_c and M−O_t bond orders. The Mayer and covalency indexes for the O_t atoms are smaller for the Nb and Ta anions (than for the Mo and W clusters), and this corresponds with greater values for the O_c atoms.

Table 11. Fragment Analysis for Oxidized Anions (Energy Terms in eV)

term	atom	$[Nb_6O_{19}]^{8-}$	$[Ta_6O_{19}]^{8-}$	$[Mo_6O_{19}]^{2-}$	$[W_6O_{19}]^{2-}$
ΔE_B	O_c	+19.94	+19.97	−20.20	−20.77
	O_b	+18.76	+18.78	−21.21	−22.17
	O_t	+17.16	+17.13	−21.62	−22.45
ΔE_O	O_c	−12.65	−12.34	−12.25	−12.77
	O_b	−14.02	−13.60	−15.96	−16.30
	O_t	−12.95	−12.56	−18.01	−17.67
Δe_o	O_c	−2.11	−2.06	−2.04	−2.13
	O_b	−7.01	−6.80	−7.98	−8.15
	O_t	−12.95	−12.56	−18.01	−17.67

Fragment Analysis. A fragment-decomposition analysis based on eq 2 can provide a further measure of the relative bonding capacity and strength of central, bridging, and terminal sites in the $[M_6O_{19}]^{n-}$ polyanions. The clusters can be described as

$$[M_6O_{18}]^{(6-)/(0)} + [O]^{(2-)} = [M_6O_{19}]^{(8-)/(2-)} \quad (4)$$

and the total molecular bonding energy relative to the fragments is then given by

$$\Delta E_B = \Delta E_O + \Delta E_P + \Delta E_E \quad (5)$$

The orbital-interaction contribution can be normalized as Δe_o by calculating

$$\Delta e_o = \frac{\Delta E_O}{n} \quad (6)$$

where n is the number of additional bonds in the molecule with respect to the uncombined fragments.

The results from eqs 4−6 are summarized in Table 11. It is evident that the large charge differences between Nb/Ta and Mo/W systems have a strong influence on the bonding stability as reflected by the completely opposite ΔE_B values. Nevertheless, it is important to note the similarities in the results for the various O atoms that, as the full-valency indexes do, indicate that the bonding contributions from each oxygen type are comparable, despite the rather different nature of the individual M−O interactions.

If each anion is considered separately, the Δe_o values are found to display a correlation with the Mayer bond orders but are rather sensitive to charge-redistribution effects, and it is not possible to use them for a direct comparison of different species. The ΔE_O terms also correlate with the covalency indexes, and these results suggest that, for $[Mo_6O_{19}]^{2-}$ and $[W_6O_{19}]^{2-}$, although ionic effects are somewhat more significant for O_c (than O_b or O_t) atoms, the covalent character of M−O_c bonding is appreciable, and the central-oxygen site thus appears to be considerably different from an O^{2-} entity.

As discussed in the Electronic Structure section, no particularly outstanding effects from bonds to O_b atoms are observed. In the $[M_6O_{19}]^{n-}$ polyanions, the structural stability derived from M−O_b orbital interactions may be greater than

the contributions from central and terminal bonds as a result of the number of bridging bonds being (much) greater but, apparently, not because these are distinctively stronger.

Conclusion

The molecular and electronic structures of $[M_6O_{19}]^{n-}$ isopolyanions have been investigated using density-functional methods. Good computational−experimental agreement has been obtained for the geometrical parameters of Mo and W species, but important discrepancies have occurred in the results for Nb and Ta clusters, probably as a consequence of the high negative charge of these molecules.

The molecular orbital and population analysis have indicated that the M−O interactions are largely of M d−O p character and can be characterized as (fractional) multiple terminal bonds, approximately single bridging bonds, and low-order central bonds, in accord with bond-valence and structural data. Bonds of σ and π nature are formed between the metal centers and the terminal and bridging oxygen atoms. Some of these bonds, including the LUMO of oxidized anions, can be described in terms of the $[M_4O_4]$ closed loops proposed by Nomiya and Miwa. The valency and bonding-energy results have revealed similarities in the overall bonding capacity and strength of the various oxygen sites, and the latter have not indicated that there is a special stabilizing contribution associated with the $[M-O_b]$ closed loops.

Minimal structural changes have been detected on reduction of molybdates and tungstates. This result is consistent with the general properties of the orbitals occupied by the added electrons. These orbitals have been found not to strongly affect the stability of the polyanions being only slightly antibonding and to be extensively delocalized over the $[M-O_b]$ network.

The Mulliken analysis has yielded a distribution of the negative charge over all types of oxygen sites and has suggested that some structural changes in the reduced species may be closely connected with repulsions on the polyanion surface, as the excess charge tends to accumulate on O_t and, to a lesser extent, O_b atoms. The metal charges have been found to be considerably smaller than the formal oxidation states.

Acknowledgment. The authors thank the EPSRC, the Cambridge Overseas Trust, Selwyn College (Cambridge, U.K.), and the University of Hull for financial support and the Computational Chemistry Working Party for access to computational facilities in the Rutherford Appleton Laboratory.

Supporting Information Available: Listings of calculated O−M−O and M−O−M angles for oxidized anions. This material is available free of charge via the Internet at http://pubs.acs.org.

IC011086F